Magnetic and magnetocaloric properties of $HoCr_{0.75}Fe_{0.25}O_3$ compound

Ganesh Kotnana[1], P. D. Babu[2] and S. Narayana Jammalamadaka[1*]

[1]*Magnetic Materials and Device Physics Laboratory, Department of Physics, Indian Institute of Technology Hyderabad, Hyderabad, India – 502 285.*

[2]*UGC-DAE Consortium for Scientific Research, Mumbai Centre, BARC Campus, Mumbai, India – 400 085.*

*Corresponding author: surya@iith.ac.in

Abstract:

We report on the magnetic and magnetocaloric properties of $HoCr_{0.75}Fe_{0.25}O_3$ compound around the Néel temperature (T_N), which is due to Cr^{3+} ordering. Susceptability (χ) *vs.* temperature (T) graph of $HoCr_{0.75}Fe_{0.25}O_3$ compound infer two transitions due to the ordering of Cr^{3+} moments ($T_N \sim 155$ K) and Ho^{3+} moments ($T_N^{Ho} \sim 8$ K). Magnetic entropy ($-\Delta S_M$) value of 1.14 J kg^{-1} K^{-1} around 157.5 K with a magnetic field (H) of 90 kOe is attributed to antiferromagnetic (AFM) ordering of Cr^{3+} moments. A maximum value of adiabatic temperature (ΔT_{ad}) ~ 0.41 K around T_N is obtained and is found to increases with applied magnetic field. Negative slope for H/M *vs.* M^2 graph is evident for $HoCr_{0.75}Fe_{0.25}O_3$ compound below T_N, which indicates the first order phase transition. Quantified values of $-\Delta S_M$ and ΔT_{ad} opens up the way to explore rare earth orthochromites for the MCE properties and refrigeration applications.

Key words: Magnetocaloric effect, magnetization, specific heat, orthochromite

Introduction:

In recent years, there has been growing interest in search of new materials and technologies for refrigeration applications both at room temperature as well as at cryogenic temperatures using magnetocaloric effect (MCE) phenomenon. Refrigeration using the magnetocaloric materials have significant advantages such as higher energy efficiency and environmental safety over the conventional gas compression techniques [1-3]. MCE is a magneto-thermal phenomenon, which is associated with a change in the temperature of a magnetic material when it is exposed to external magnetic field adiabatically [4]. A magnetic material with a large change of magnetic entropy $\Delta S_M(T,H)$, adiabatic temperature change (ΔT_{ad}) and a sufficiently large value of refrigeration capacity (RC) has been promising candidate for magnetic refrigeration [5]. The perovskite oxides with general formula ABO_3 have been studied for the MCE properties using three methods, (a) calculation of $-\Delta S_M$ from the isothermal magnetization using Maxwell's relation [6-7] (b) heat capacity C_p measurements [8-10] and (c) direct measurement of the adiabatic temperature change by exposing thermally insulated sample to the magnetic field [11-13].

Magnetic contribution to the specific heat (C_p) can be obtained from the total C_p after subtracting the electronic and phonon contribution [14]. In general, the materials with smaller C_p values are desirable for the refrigeration application as ΔT_{ad} is inversely proportional to C_p [15]. Rare earth orthochromites with chemical formula $RCrO_3$, have drawn considerable attention due to their distinctive magnetic, ferrolectric and magnetoelectric properties [16-18]. Apart from the above, unique features such as negative magnetization, exchange bias and magnetization switching have been reported on orthochromites [17, 19-21]. As $RCrO_3$ compounds show smaller C_p values (~ 95 - 109 J mol^{-1} K^{-1}) and consequently larger ΔT_{ad} values, these compounds have been of great interest for the MCE applications [9, 22-24]. For

example, a larger value of $-\Delta S_M \sim 8.4$ J kg^{-1} K^{-1} and RC ~ 217 J kg^{-1} at 15 K and 40 kOe have been observed in $DyCrO_3$ due to ordering of Dy^{3+} [22]. Yin *et.al,* have reported $-\Delta S_M \sim 10.5$ J kg^{-1} K^{-1} at 40 kOe around Dy^{3+} ordering (14 K) in $DyFe_{0.5}Cr_{0.5}O_3$ compound [23]. Yet in another compound, $HoCrO_3$, a large value of $-\Delta S_M \sim 7.2$ J kg^{-1} K^{-1} and RC ~ 408 J kg^{-1} at 20 K have been reported at 70 kOe [24]. In the present work, we explored magnetic and MCE properties of $HoCr_{0.75}Fe_{0.25}O_3$ compound for refrigeration applications.

Experimental Details:

Polycrystalline $HoCr_{0.75}Fe_{0.25}O_3$ compound was prepared by conventional solid state reaction method using High purity oxide powders of Ho_2O_3, Fe_2O_3, and Cr_2O_3 (purity > 99.9%) (Sigma-Aldrich chemicals India) as starting raw materials. The mixture thus obtained was thoroughly and repeatedly ground in the isopropanol alcohol using the agate mortar and pestle to ensure homogeneity. Pellets were prepared using the resultant powder and sintered sequentially at 1000^{o}C for 12 h, 1200^{o}C for 12 h and 1250^{o}C for 24 h respectively. The temperature (T) dependent magnetization (M) (M *vs.* T) and magnetic field (H) dependent magnetization (M *vs.* H) measurements were performed using a Quantum Design magnetic property measurement system (MPMS) in the temperature range of 5 – 300 K. Magnetization isotherms (M *vs.* H) were measured at different temperature ranges and up to a maximum magnetic field of 90 kOe. Before we perform each measurement of M *vs.* H, the sample was warmed up to a temperature greater than ordering temperature of transition metal to remove the magnetic history. Quantum design physical property measurement system (PPMS) was used for the Cp measurement (Relaxation method).

Results and Discussion:

Fig. 1(a) and (b) depicts the XRD patterns of HoCrO3 and $HoCr_{0.75}Fe_{0.25}O_3$ compounds respectively. Phase purity of $HoCr_{0.75}Fe_{0.25}O_3$ compound is determined at room temperature

using a powder x - ray diffraction (XRD) (PANalytical X-ray diffractometer) with Cu - K_α radiation (λ = 1.5406 Å) and with a step size of 0.017^o in the wide range of the Bragg's angle 2θ (20^0 - 80^0) and is shown in Fig 1(b). Rietveld refinement was performed on the obtained XRD patterns of $HoCrO_3$ and $HoCr_{0.75}Fe_{0.25}O_3$ compounds using GSAS software [25]. It is evident from the refinement data that both the compounds are formed in orthorhombic structure with a space group of Pbnm. Extracted lattice parameter value is found to change by the addition of Fe^{3+} ion to Cr^{3+} ion. Compared with $HoCrO_3$ (a = 5.25009Å, b = 5.51635 Å and c = 7.54373 Å) compound, an increase in lattice parameter is observed for $HoCr_{0.75}Fe_{0.25}O_3$ (a = 5.25658 Å, b = 5.53709 Å and c = 7.55790 Å) compound due to larger ionic radii of Fe^{3+} (0.645 Å) [26] in comparison with the Cr^{3+} (0.615 Å) [26] ion.

Fig. 1(c) depicts the temperature (T) dependence of dc magnetic susceptibility (χ) of $HoCr_{0.75}Fe_{0.25}O_3$ compound recorded at a magnetic field of 1000 Oe under zero field cooled (ZFC) and field cooled (FC) conditions. An increase in χ with a decrease in temperature from 300 K up to a characteristic temperature, namely Néel temperature (T_N) ~ 155 K is evident as shown in Fig. 1(c), due to antiferromagnetic (AFM) ordering of Cr^{3+} moments (peak expanded for clarity) [27]. Below T_N, χ behaviour is quite different and diamagnetism like negative magnetization is observed in ZFC curve. Similar behaviour has been observed by Su Yuling *et. al.*, on $HoCrO_3$ compound, and explained on the basis of competing weak ferromagnetism (WFM) – AFM interactions [28]. However, one of the problems with ZFC magnetization measurement usually encountered is a small negative trapping field in the sample space, which is responsible for the observed negative magnetization of ferro/ferri/antiferromagnetic materials [29]. Contrary to our observation, the Neutron diffraction study on $HoFe_{1-x}Cr_xO_3$ solid solutions reveral that there is no signature of negative magnetization [30]. As stated above, the observed negative magnetization may be due to trapped fields. Apart from T_N (due to Cr^{3+} transition), transition due to Ho^{3+} moments is

evident at 8 K (T_N^{Ho}), which is in accordance with the literature value [28]. The corresponding dM/dT *vs.* T graph of field cooled (FC) M *vs.* T data is shown as an inset of Fig. 1(c).

The variation of the specific heat (C_p) of $HoCr_{0.75}Fe_{0.25}O_3$ compound in the temperature range between 100 - 200 K was recorded with zero magnetic field and by varying magnetic field strengths 30 kOe, 50 kOe and 70 kOe respectively (Fig 2(a)). The shape of C_p *vs.* T is generally consistent with the results of prior work on orthochromites such as $NdCrO_3$ [31] and $YbCrO_3$ [32]. It is seen from the Fig. 2(a) that C_p decreases with decrease in temperature and a λ-shape anomaly is evident at around $T_N \sim 155$ K in the case of $HoCr_{0.75}Fe_{0.25}O_3$ compound. This anomaly is associated with a paramagnetic to canted antiferromagnetic (AFM) phase transition [28]. The value of C_p is found to be 83.8 J mol^{-1} K^{-1} at 200 K from the C_p *vs.* T data recorded under zero magnetic field (0 Oe), which is almost equal to the value of C_p pertinent to $HoCrO_3$ (83.3 J mol^{-1} K^{-1} at 200 K) compound [9]. To extract the magnetic heat capacity C_{mag} pertinent to AFM ordering, a third order polynomial background is subtracted from the experimental C_p *vs.* T data which is obtained at 0 Oe in order to exclude the electron and phonon contribution as shown in Fig 2(b). Similar treatment is done for the data (C_p *vs.* T) under different magnetic field strengths 30 kOe, 50 kOe and 70 kOe respectively. The excess heat capacity due to AFM transition at different magnetic fields (0 Oe, 30 kOe, 50 kOe and 70 kOe) in the temperature range between 100 and 200 K is plotted as C_{mag} *vs.* T and is presented in Fig 2(c). Significant change in the value of C_p (H, T) is not evident up to the maximum magnetic field of 70 kOe. The magnetic heat capacity C_{mag}/T *vs.* T data at 0 Oe is used to calculate the magnetic entropy associated with magnetic transition using the equation

$$S_{mag} = \int_{T_1}^{T_2} \left(\frac{C_{mag}}{T} \right) dT \qquad \ldots\ldots (1)$$

and is shown in Fig. 2(d). The calculated S_{mag} is 1.21 J mol^{-1} K^{-1} and is well below the expected full spin entropy, $S_{mag} = R\ln(2S+1)$ where S (3/2) is the spin of Cr^{3+} ions in the samples, and R is the molar gas constant.

In order to calculate the magnetic entropy associated with Cr^{3+} ordering, isothermal M *vs.* H loops were recorded around T_N as shown in Fig. 3(a). It is evident from the Figure that low field nonlinearity is due to weak ferromagnetic (WFM) component which arises due to canting of Cr^{3+} moments. Apart from that, an increase in linearity of M *vs.* H curves is evident with an increase in temperature from 100 K up to T_N (155 K) due to decrease in strength of WFM component. The disappearance of nonlinearity for M *vs.* H curves above T_N indicates the paramagnetic phase. The magnetic entropy change ($-\Delta S_M$) is estimated using isothermal M *vs.* H curves and by the Maxwell's relation:

$$\Delta S_M(T,H) = \int_0^{H_{max}} \left(\frac{\partial M}{\partial T}\right)_H dH \qquad \ldots\ldots (2)$$

where H_{max} is the maximum value of external applied magnetic field.

From the above Eq. (2), it can be noticed that the value of $-\Delta S_M$ depends on both values of magnetization (M) and $\left(\frac{\partial M}{\partial T}\right)_H$. The larger values of $-\Delta S_M$ can be obtained when the values of M and $\left(\frac{\partial M}{\partial T}\right)_H$ are large in the magnitude [33]. Fig. 3(b) depicts the quantified values of $-\Delta S_M$ and its temperature variation. Evidenced $-\Delta S_M$ value of 1.14 J kg^{-1} K^{-1} around 157.5 K with a magnetic field of 90 kOe is attributed to AFM ordering of Cr^{3+} moments. The value of $-\Delta S_M$ = 0.45 J kg^{-1} K^{-1} at T_N with 50 kOe in the present study is large compared to other chromites such as $YbCrO_3$ (0.41 J kg^{-1} K^{-1}) [34], $YCrO_3$ (0.36 J kg^{-1} K^{-1}) [34] and $SmCrO_3$ (0.15 J kg^{-1} K^{-1}) [34]. A decrease in $-\Delta S_M$ value has been evident for $HoCr_{0.75}Fe_{0.25}O_3$ (0.59 J

$kg^{-1} K^{-1}$ at 157.5 K with 60 kOe) compound in comparison with the $HoCrO_3$ (1.05 J $kg^{-1} K^{-1}$ at 141 K with 60 kOe) compound [35]. Magnetic entropy change of 1.14 J/kgK is observed at Néel temperature (157. 5 K) at 90 kOe. In addition, as it is evident from χ vs. T, the susceptibility increases (and hence the magnetization) up to the temperatures as low as 2 K (Fig. 1(c)). As MCE is directly proportional to the magnetization, we do see an increase in $-\Delta S_M$ below T_N. The origin of increase in magnetization is attributed the molecular field of Cr^{3+} moments, which may order the Ho^{3+} moments.

It is well known that magnetic materials with large value of $-\Delta S_M$ and ΔT_{ad} are needed for refrigeration application [5]. It is well known that under adiabatic conditions magnetic material will cool down by inducing an adiabatic temperature change ΔT_{ad}. According to Maxwell's relation, ΔT_{ad} associated with magnetic transition and can be calculated using the following equation:

$$\Delta T_{ad} = -\int_0^H \frac{T}{Cp(T,H)}\left(\frac{\partial M}{\partial T}\right)_H dH = -\Delta S_M \left(\frac{T}{Cp(T,H)}\right) \quad \ldots\ldots (3)$$

where $-\Delta S_M$ is magnetic entropy change deduced from the isothermal magnetic measurements and C_p is the total specific heat value. According to Eq. (3), a large value of ΔT_{ad} can be expected to occur around PM - AFM transition since the rate of change of magnetization is large with temperature. However, the magnitude of C_p at that transition also plays a crucial role in determining the cooling efficiency of the material, as it varies significantly from one magnetocaloric material family to other. For example, the heat capacity of a Gd-based alloy system is much smaller than that of a manganite type material system [36]. Therefore, a reliable comparison of the efficiency of different magnetocaloric materials should be based on evaluating ΔT_{ad} instead of $-\Delta S_M$. The variation of ΔT_{ad} with respect to the magnetic field H around AFM ordering (T_N) is shown in Fig. 3(c). It is evident

that the value of ΔT_{ad} increases with increase of applied magnetic field, and reaches a maximum value of 0.41 K around T_N. The value of ΔT_{ad} for the present compound (0.11 K at T_N ~155 K with 30 kOe) is found larger in comparison with $SmCrO_3$ (ΔT_{ad} = 0.03 K at T_N ~ 192 K with 30 kOe) compound [37].

In order to investigate the nature of H or T induced magnetic transition near T_N, isothermal M *vs.* H curves are plotted in the form of Arrott plots (H/M *vs.* M^2) [38] and are shown in Fig. 3(d). The sign (positive or negative) of the slope of Arrott plot describes the kind of magnetic phase transition. According to Banerjee's criterion [39], the first order phase transition yields a negative slope while the second order phase transition yields a positive slope for Arrott plot. From the Fig 3(d), negative slope for H/M *vs.* M^2 is evident at lower values of M^2 for $HoCr_{0.75}Fe_{0.25}O_3$ compound below T_N indicates the first order phase transition.

Conclusions:

In conclusion, the room temperature powder XRD pattern confirmed the phase purity of the $HoCr_{0.75}Fe_{0.25}O_3$ compound. χ *vs.* T graph of $HoCr_{0.75}Fe_{0.25}O_3$ compound infer two transitions due to Cr^{3+} moments (T_N ~ 155 K) and Ho^{3+} (T_N^{Ho} ~ 8 K) moments respectively. As the change in ΔT_{ad} ~ 0.41 K is large around Cr^{3+} ordering, we believe that $HoCr_{0.75}Fe_{0.25}O_3$ compound may be potential candidate for magnetic refrigeration applications.

Acknowledgements

We would like to acknowledge Indian Institute of Technology, Hyderabad and Department of Science and Technology (DST) **(**Project #SR/FTP/PS-190/2012**)** for the financial support. We are grateful to UGC-DAE Consortium (Project # CSR-IC/CRS-162/2015-16/19) for the financial support.

References:

[1] Gschneidner Jr K. A, Pecharsky V. K and Tsokol A. O, *Rep. Prog. Phys.* **68**, 1479 (2005).

[2] Gutfleisch O,Willard M A, Bruck E, Chen C H, Sankar S G and Liu J P, *Adv. Mater.* **23**, 821 (2011).

[3] Shen B G, Sun J R, Hu F X, Zhang H W and Cheng Z H, *Adv. Mater.* **21**, 4545 (2009).

[4] N. S. Bingham, H. Wang, F. Qin, H. X. Peng, J. F. Sun, V. Franco, H. Srikanth and M. H. Phan, *Appl. Phys. Lett.* **101**, 102407 (2012).

[5] Ling-Wei Li, *Chinese Phys. B* **25**, 037502 (2016).

[6] Shiqi Yin, Mohindar S. Seehra, Curtis J. Guild, Steven L. Suib, Narayan Poudel, Bernd Lorenz, and Menka Jain, *Phys. Rev.* **B** 95, 184421 (2017).

[7] Mohit K. Sharma, Tathamay Basu, K. Mukherjee, and E. V. Sampathkumaran, *J. Phys.: Condens. Matter* **28**, 426003 (2016).

[8] A. Duran, A. M. Arevalo-Lopez, E. Castillo-Martinez, M. Garcia-Guaderrama, E. Moran, M. P. Cruz, F. Fernandez, and M. A. Alario-Franco, *J. Solid State Chem.* **183**, 1863 (2010).

[9] Hirohisa Satoh, Shin-ichi Koseki, Masaki Takagi, Won Yang Chung, and Naoki Kamegashira, *J. Alloys Compd.* **259**, 176 (1997).

[10] Yi Du, Zhen Xiang Cheng, Xiao-Lin Wang, and Shi Xue Dou, *J. Appl. Phys.* **108**, 093914 (2010).

[11] A. Rostamnejadi, M. Venkatesan, P. Kameli, H. Salamati, J. M. D. Coey, *J. Magn. Magn. Mater.* **323**, 2214 (2011).

[12] Charlotte Mayer, Stephane Gorsse, Geraldine Ballon, Rafael Caballero-Flores, Victorino Franco, and Bernard Chevalier, *J. Appl. Phys.* **110**, 053920 (2011).

[13] S. Gorsse, C. Mayer, and B. Chevalier, *J. Appl. Phys.* **109**, 033914 (2011).

[14] K. Saito, A. Sato, A. Bhattacharjee, and M. Sorai, *Solid State Commun.* **120**(4), 129–132 (2001).

[15] M. M. Vopson, *J. Phys. D. Appl. Phys.* **46**, 345304 (2013).

[16] A. Jaiswal, R. Das, K. Vivekanand, T. Maity, P. M. Abraham, S. Adyanthaya, and P. Poddar, *J. Appl. Phys.* **107**, 013912 (2010).

[17] P. Gupta, R. Bhargava, R. Das, and P. Poddar, *RSC Adv.* **3**, 26427 (2013).

[18] J. R. Sahu, C. R. Serrao, N. Ray, U. V. Waghmare and C. N. R. Rao, *J. Mater. Chem.* **17**, 42 (2007).

[19] P. Gupta, R. Bhargava, and P. Poddar, *J. Phys. D. Appl. Phys.* **48**, 025004 (2015).

[20] P. K. Manna and S. M. Yusuf, *Phys. Rep.* **535**, 61 (2014).

[21] A. Kumar, and S. M. Yusuf, *Phys. Rep.* **556**, 1 (2015).

[22] A. McDannald, L. Kuna and M. Jain, *J. Appl. Phys.***114,** 113904 (2013).

[23] L. H. Yin, J. Yang, R. R. Zhang, J. M. Dai, W. H. Song and Y. P. Sun, *Appl. Phys. Lett.* **104**, 032904 (2014).

[24] S. Yin and M. Jain, *J. Appl. Phys.* **120**, 043906 (2016).

[25] Ganesh Kotnana and S. Narayana Jammalamadaka, *J. Appl. Phys.* **118**, 124101 (2015).

[26] R. D. Shannon, Acta Crystallogr., Sect. **A** 32, 751 (1976).

[27] Ganesh Kotnana, V. Raghavendra Reddy, and S. Narayana Jammalamadaka, *J. Magn. Magn. Mater.* **429**, 353 (2017).

[28] Su Yuling, Zhang Jincang, Feng Zhenjie, Li Zijiong, Shen Yan, Cao Shixun, *J. Rare Earths* **29**, 1060 (2011).

[29] N. Kumar and A. Sundaresan, *Solid State Commun.* **150**, 1162 (2010).

[30] Xinzhi Liu, Lijie Hao, Yuntao Liu, Xiaobai Ma, Siqin Meng, Yuqing Li, Jianbo Gao, Hao Guo, Wenze Han, Kai Sun, Meimei Wu, Xiping Chen, Lei Xie, Frank Klose, Dongfeng Chen, *J. Magn. Magn. Mater.* **417**, 382 (2016).

[31] F. Bartolome, J. Bartolome, M. Castro, and J. J. Melero, *Phys. Rev.* **B** 62, 1058 (2000).

[32] Y.Su, J. Zhang, Z. Feng, L. Li, B. Li, Y. Zhou, Z. Chen and S. Cao, *J. Appl. Phys.* **108**, 013905 (2010).

[33] Zhong Wei, Au Chak-Tong, and Du You-Wei, *Chin. Phys. B* **22**, 057501 (2013).

[34] Goncalo Oliveira, thesis "Local probing spinel and perovskite complex magnetic systems" (2017).

[35] Ganesh Kotnana, Dwipak Prasad Sahu, and S. Narayana Jammalamadaka, *J. Alloys Compd.* 709, 410 (2017).

[36] K. A. Gschneidner Jr, V. Pecharsky, A. Tsokol, *Rep. Prog. Phys.* **68**, 1479 (2005).

[37] Preeti Gupta, and Pankaj Poddar, *RSC Adv.* 6, 82014 (2016).

[38] Arrott A, *Phys. Rev.* **108**, 1394 (1957).

[39] S. K. Banerjee, *Physics Letters* **12**, 16 (1964).

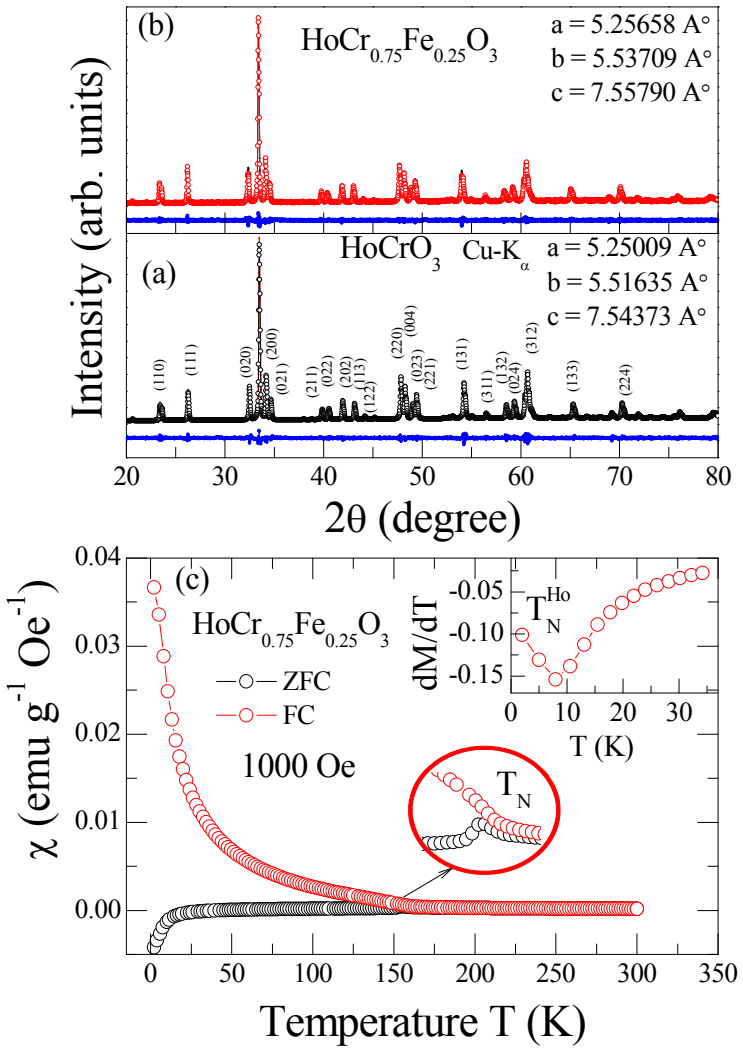

Fig. 1: Powder x-ray diffraction pattern recorded at room temperature pertinent to (a) HoCrO3 and (b) $HoCr_{0.75}Fe_{0.25}O_3$ compound. (c) Temperature dependence of susceptibility pertinent to $HoCr_{0.75}Fe_{0.25}O_3$ compound. Region pertinent to T_N expanded for clarity. Inset of Fig. 1(c) shows the first derivative of field cooled (FC) M *vs.* T curve.

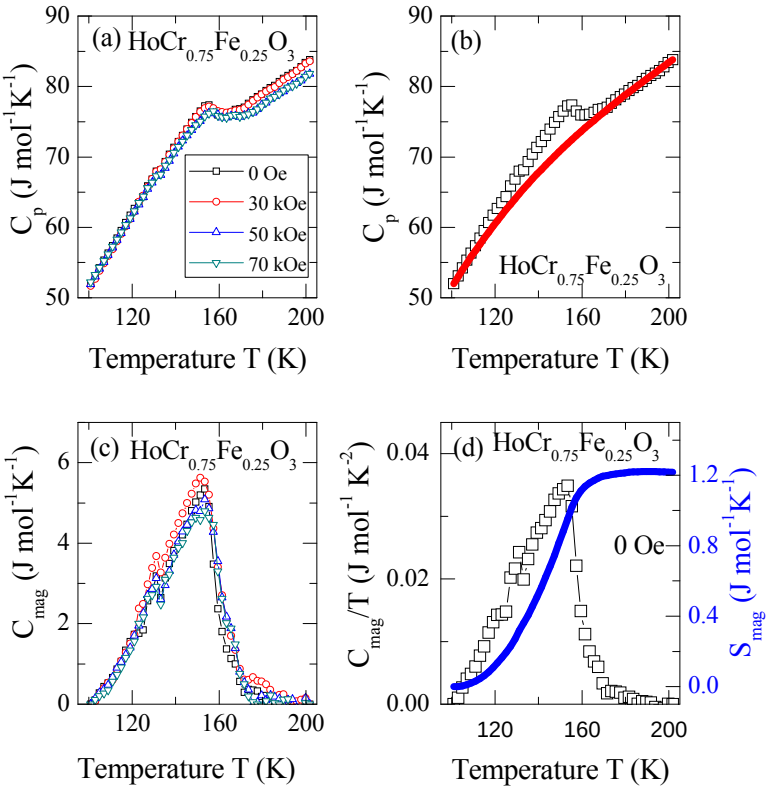

Fig. 2: (a) Variation of specific heat C_p with temperature (T) at different magnetic fields (b) subtraction of phonon and electron contribution using third order polynomial from the specific heat data. Fitted data is shown as red line and experimental data is shown as black square symbols (c) temperature dependence of C_{mag} variation around Cr^{3+} ordering at different magnetic fields (d) variation of C_{mag}/T and S_{mag} with temperature for $HoCr_{0.75}Fe_{0.25}O_3$ compound.

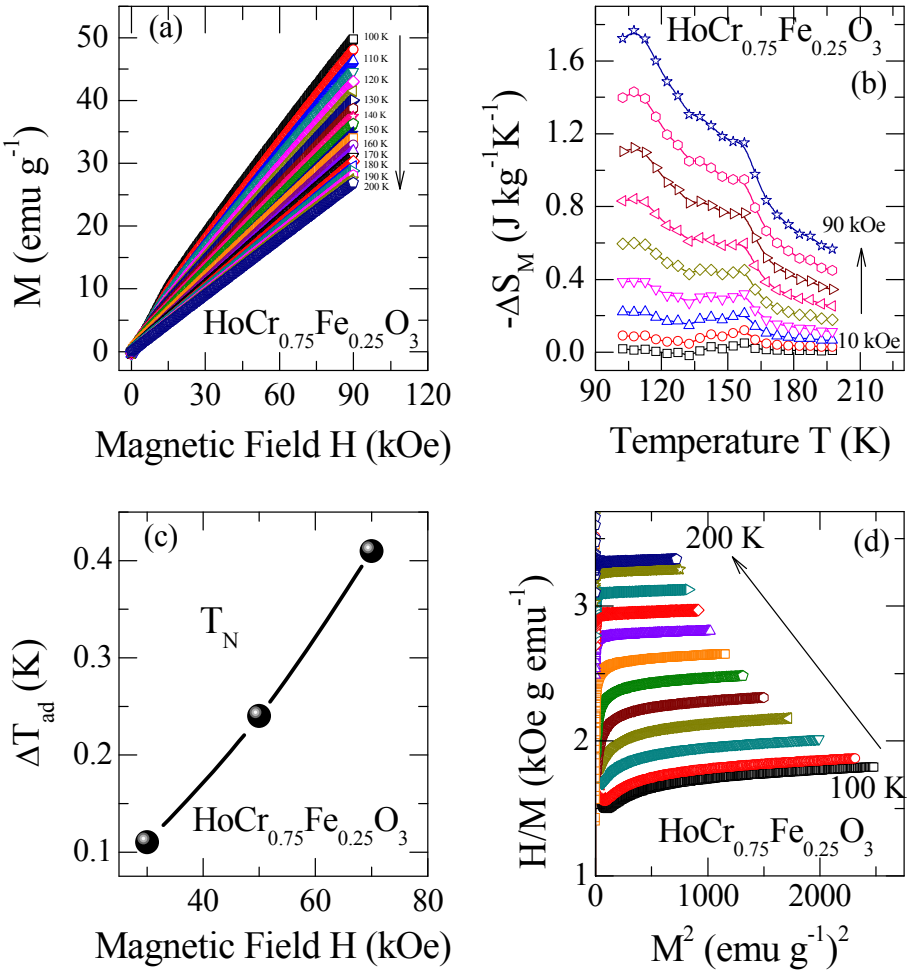

Fig. 3: (a) Isothermal magnetization (M) *vs.* magnetic field (H) curves in the temperature range 100 – 200 K (b) Temperature dependent magnetic entropy change $-\Delta S_M$ in the field range 10 – 90 kOe (c) variation of adiabatic temperature change ΔT_{ad} with magnetic field (d) Arrott plots corresponding to isothermal M *vs.* H curves for $HoCr_{0.75}Fe_{0.25}O_3$ compound.